Magnetic-Assisted, Self-Healable, Yarn-Based Supercapacitor

Yang Huang,[†,⊥] Yan Huang,[†,⊥] Minshen Zhu,[†] Wenjun Meng,[†] Zengxia Pei,[†] Chang Liu,[‡] Hong Hu,[*,‡] and Chunyi Zhi[*,†,§]

[†]Department of Physics and Materials Science, City University of Hong Kong, 83 Tat Chee Avenue, Kowloon, Hong Kong 999077, China, [‡]Institute of Textiles and Clothing, The Hong Kong Polytechnic University, 11 Hong Chong Road, Hung Hom, Hong Kong 999077, China, and [§]Shenzhen Research Institute, City University of Hong Kong, 8 Yuexing Yi Road, Nanshan, Shenzhen 518000, China. [⊥]Yang Huang and Yan Huang contributed equally to this work.

ABSTRACT

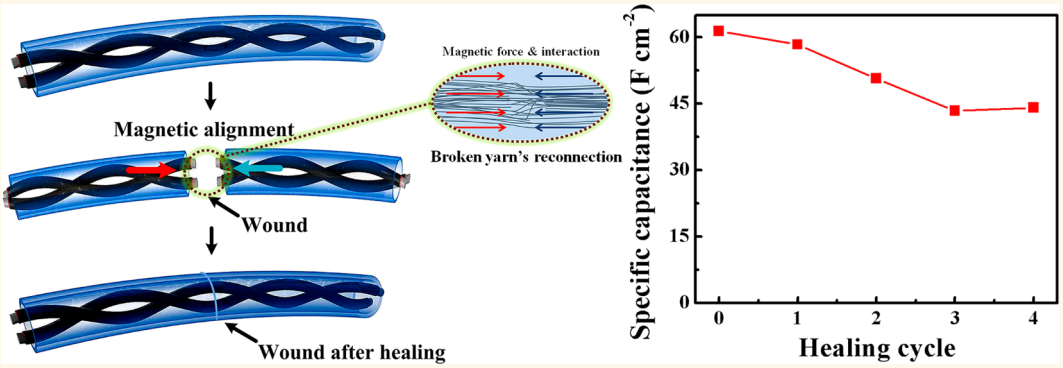

Yarn-based supercapacitors have received considerable attention recently, offering unprecedented opportunities for future wearable electronic devices (*e.g.*, smart clothes). However, the reliability and lifespan of yarn-based supercapacitors can be seriously limited by accidental mechanical damage during practical applications. Therefore, a supercapacitor endowed with mechanically and electrically self-healing properties is a brilliant solution to the challenge. Compared with the conventional planar-like or large wire-like structure, the reconnection of the broken yarn electrode composed of multiple tiny fibers (diameter <20 μm) is much more difficult and challenging, which directly affects the restoration of electrical conductivity after damage. Herein, a self-healable yarn-based supercapacitor that ensures the reconnection of broken electrodes has been successfully developed by wrapping magnetic electrodes around a self-healing polymer shell. The strong force from magnetic attraction between the broken yarn electrodes benefits reconnection of fibers in the yarn electrodes during self-healing and thus offers an effective strategy for the restoration of electric conductivity, whereas the polymer shell recovers the configuration integrity and mechanical strength. With the design, the specific capacitance of our prototype can be restored up to 71.8% even after four breaking/healing cycles with great maintenance of the whole device's mechanical properties. This work may inspire the design and fabrication of other distinctive self-healable and wearable electronic devices.

KEYWORDS: magnetic-assisted · self-healable · yarn · supercapacitor

Wearable energy-storage devices are increasingly demanded because of the popularization of personalized electronics.[1−6] Yarn-based supercapacitors have become a promising class of such wearable energy-storage devices for their high power density, fast rate of charge−discharge, long cycle lifetimes, and good compatibility with traditional textile.[7−10] Recently, considerable efforts have been dedicated to developing novel electrode materials with higher capacitive performance and unique miniaturized configurations with greater compatibility, in accordance with the trend of the development of wearable supercapacitors.[11−19] However, in their long life cycles, these delicate supercapacitors inevitably suffer from all kinds of local stress under bending or other deformations, which is a common problem for wearable electronics during practical applications. This may cause permanent mechanical failure over time. The unavoidable failures would seriously limit the lifespan and reliability of the supercapacitor, resulting in a malfunction of the

* Address correspondence to tchuhong@polyu.edu.hk, cy.zhi@cityu.edu.hk.

Received for review March 15, 2015 and accepted June 1, 2015.

Published online June 01, 2015
10.1021/acsnano.5b01602

whole device.[20−23] Consequently, a perfect yarn-based supercapacitor should not only present superior electrochemical performance but also retain mechanical and electrical sustainability for practical applications. Considering the obvious omissions of the sustainability in current research, it is of great realistic significance to develop ideal supercapacitors with the capability for damage management. Besides, it is even better if the supercapacitor could be endowed with additional properties, for example, the capability to restore both mechanical and electrical properties automatically after mechanical damage.

Self-healing materials, which are able to heal and repair damages autonomically or in response to external stimuli such as changes in pH, heat, or light,[24,25] have been successfully developed in the past decade. On this basis, self-healable supercapacitors have been recently fabricated by employing a self-healing polymer for mechanical recovery and simultaneously realizing the restoration of the electric conductivity of the broken electrodes.[26,27] Such supercapacitors were endowed with the capability to restore the configuration integrity and electrical properties after multiple mechanical damages.[26,27] Nevertheless, compared with the conventional planar-like or large wire-like structures, ensuring the reconnection of the broken yarn-based electrode is much more challenging, since it is composed of multiple tiny fibers (diameter <20 μm). It is unrealistic to reconnect each of the tiny broken fibers combined in the yarn accurately by visual inspection. In order to achieve the restoration of electrochemical performance after damage, a good reconnection of the broken yarn in the supercapacitor is essential.

Previously, we have successfully fabricated a large-sized supercapacitor textile using a special conductive yarn, which can withstand various chemical processes, including hydrothermal synthesis and electrochemical deposition.[28] Herein, utilizing this special yarn, a magnetic-assisted mechanically and electrically self-healable yarn-based supercapacitor was developed for the first time. Our self-healable yarn-based supercapacitor is fabricated by wrapping the magnetic electrodes in a self-healable polyurethane (PU) shell. Once the supercapacitor is subjected to mechanical damage, the external movement of the self-healing shell brings the broken areas into contact and realizes mechanical self-healing autonomically, while the broken magnetic electrodes are electrically reconnected and aligned with the assistance of their own magnetic force. The synergistic effects between the self-healing shell and magnetic electrodes enable the device to restore its configuration and electrochemical performance. Up to 71.8% of the specific capacitance is recovered even after four breaking/healing cycles. Our magnetic-assisted self-healing prototype will provide a practical model and lead to next-generation wearable and robust electronic devices with an extremely long lifespan in the near future.

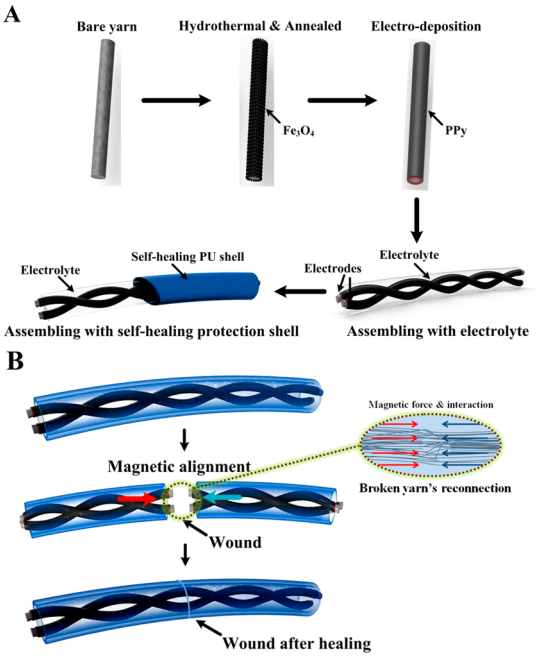

Figure 1. (A) Design and manufacturing process flow of the magnetic-assisted self-healable supercapacitor. Fe_3O_4 nanoparticles anchor on the surface of the yarn by a microwave-assisted hydrothermal method. The processed yarn is annealed to ensure the magnetic particles anchor on the yarn tightly. To achieve a better electrochemical performance, a layer of PPy is electrodeposited on the annealed yarn. Finally, two yarns as a set of electrodes are assembled with a solid electrolyte and a self-healing shell to form a self-healing supercapacitor. (B) Schematic illustration of the supercapacitor's self-healing process. The magnetic alignment could assist the reconnection of the fibers in the broken yarn electrodes when they are brought together, as shown in the inset image.

RESULTS AND DISCUSSION

Design of the Self-Healing Supercapacitor. The design and manufacturing process flow of the magnetic-assisted, self-healable, yarn-based supercapacitor is demonstrated in Figure 1A. The cleaned stainless steel yarn is treated with the microwave-assisted hydrothermal (MW-H) method several times to ensure enough magnetic Fe_3O_4 particles to nucleate and crystallize on the surface of the yarn. Afterward, the silver-colored yarn turns black, suggesting that the morphology has been changed due to the successful growth of Fe_3O_4. In order to ensure the Fe_3O_4 particles anchor firmly on the surface, the black yarn is annealed at 250 °C for 1 h. Through the treatments above, the yarn becomes magnetic, which is the key to achieve high electrical self-healing properties of the electrodes. Then, a 2 μm thick layer of polypyrrole (PPy) serving as the active material is electrodeposited on the annealed black yarn. This PPy layer not only guarantees a decent supercapacitor performance but also wraps up the Fe_3O_4 magnetic particles and protects them from

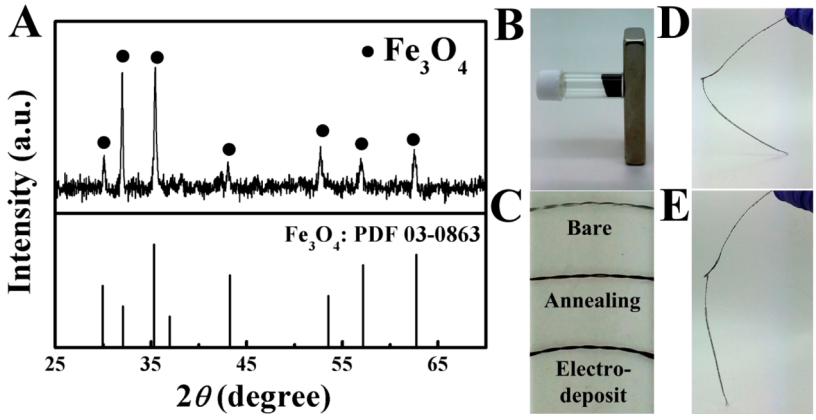

Figure 2. (A) XRD of the residual powder, which is the same material with the particles attached on the yarn after hydrothermal processes. (B) Residual powder attracted by a magnet. (C) From top to bottom, pristine yarn, hydrothermal- and annealing-treated yarn, and PPy-electrodeposited yarn. (D and E) One electrode coated with solid electrolyte is attracted by the other and pulled up by its own magnetic force. The complete process is in the Supporting Video 1.

being ripped off during applications. To fabricate an integrated supercapacitor, two electrodeposited yarns as a set of electrodes are wrapped with PVA-H_3PO_4 gel, which serves as the solid electrolyte and a separator. Last, the self-healing carboxylated PU is introduced to the outermost layer of the supercapacitor as a protection shell and makes the device self-healable. PU is selected as the outermost layer because it is self-healable, mechanically strong, and greatly compatible with the textile industry since it is often used to fabricate artificial leather. When the supercapacitor is damaged, the self-healing shell can heal the wound spontaneously.

This self-healing performance is attributed to the existence of a large amount of hydrogen bond acceptors and donors in the supramolecular network of carboxylated PU.[22,29−33] Moreover, the solid electrolyte, PVA gel, is a type of self-adhering material and can self-heal to some degree.[26,34] The two PPy-wrapped electrodes are not healable. Therefore, the magnetic electrodes are designed to solve this problem. Once the electrodes are pulled apart to be broken, as long as the separated parts are placed at suitable places, the magnetic interaction between the fibers of the yarn can guide the reconnection process, favoring the restoration of the electrical conductivity. A schematic illustration is shown in Figure 1B.

In summary, the purposes to fabricate this delicate multilayer structure are obvious: the PU shell could provide the mechanically self-healing properties, while the Fe_3O_4 magnetic layer could guarantee the restoration of electrical conductivity through the magnetic alignment. Because of its multilayer's synergistic effects, the as-assembled device should be an ideal mechanically and electrically self-healable supercapacitor.

Characterization and Morphology. First of all, in order to define the magnetic particles anchored on the yarn, the residual black powder of the MW-H method was collected and characterized by X-ray powder diffraction (XRD), in view of the fact that it should be the same particles scratched from the black hydrothermal-treated magnetic yarn. Figure 2A shows a representative XRD pattern of the as-prepared residual powders. The obvious peaks located at 30.1°, 32.0°, 35.4°, 43.1°, 53.3°, 56.9°, and 62.6° are in good agreement with magnetite (Fe_3O_4), JCPDS No. 03-0863. No other diffraction peaks were detected, revealing the high purity of the as-synthesized particles. It is well known that Fe_3O_4 exhibits permanent magnetism and is ferrimagnetic, so its powder could be easily attracted by the magnet, as shown in Figure 2B. The silver-colored yarn turns black after MW-H treatment, demonstrating that the Fe_3O_4 particles have been successfully grown on its surface. The color of the yarn shows no significant change after annealing and electrodeposition treatments, as revealed in Figure 2C, even though the morphology should have been changed. As mentioned above, the purpose of anchoring enough Fe_3O_4 on the yarn is to ensure the electrodes have enough magnetic force and assist the alignment of broken electrodes during the reconnection process. In Figure 2D,E, the strong magnetic force between two solid-electrolyte-coated electrodes is clearly demonstrated. One electrode could readily lift up the other electrode by its own magnetic force, despite the weight of the coated solid electrolyte. The complete process is shown in the Supporting Video 1. On the basis of this demonstration, it is reasonable to believe that the magnetic force between the electrodes is strong enough to assist the reconnection of broken electrodes during the self-healing process and therefore guarantees the restoration of the electrical conductivity.

As shown in Figure 3A,B, multiple stainless steel tiny fibers are twisted in a yarn and provide a large surface area, which is beneficial for both the electrical and mechanical performance. Before the treatments the

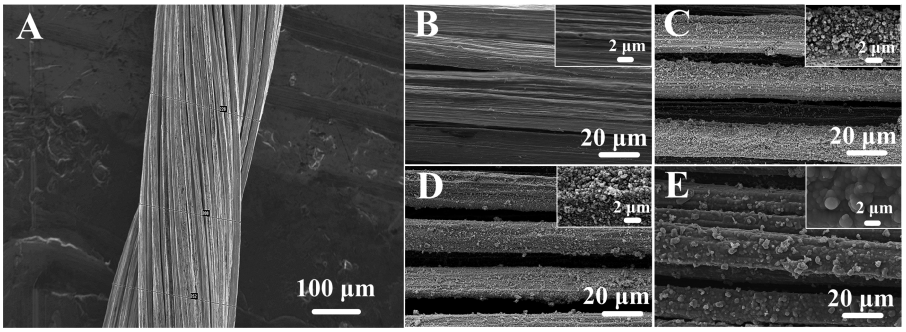

Figure 3. SEM images of the electrode after various treatments. (A) Overview image of the bare yarn consisting of twisted fibers, (B) bare fibers, (C) hydrothermal-treated fibers, (D) annealed fibers, and (E) annealed fibers electrodeposited with PPy. Insets are the high-resolution images.

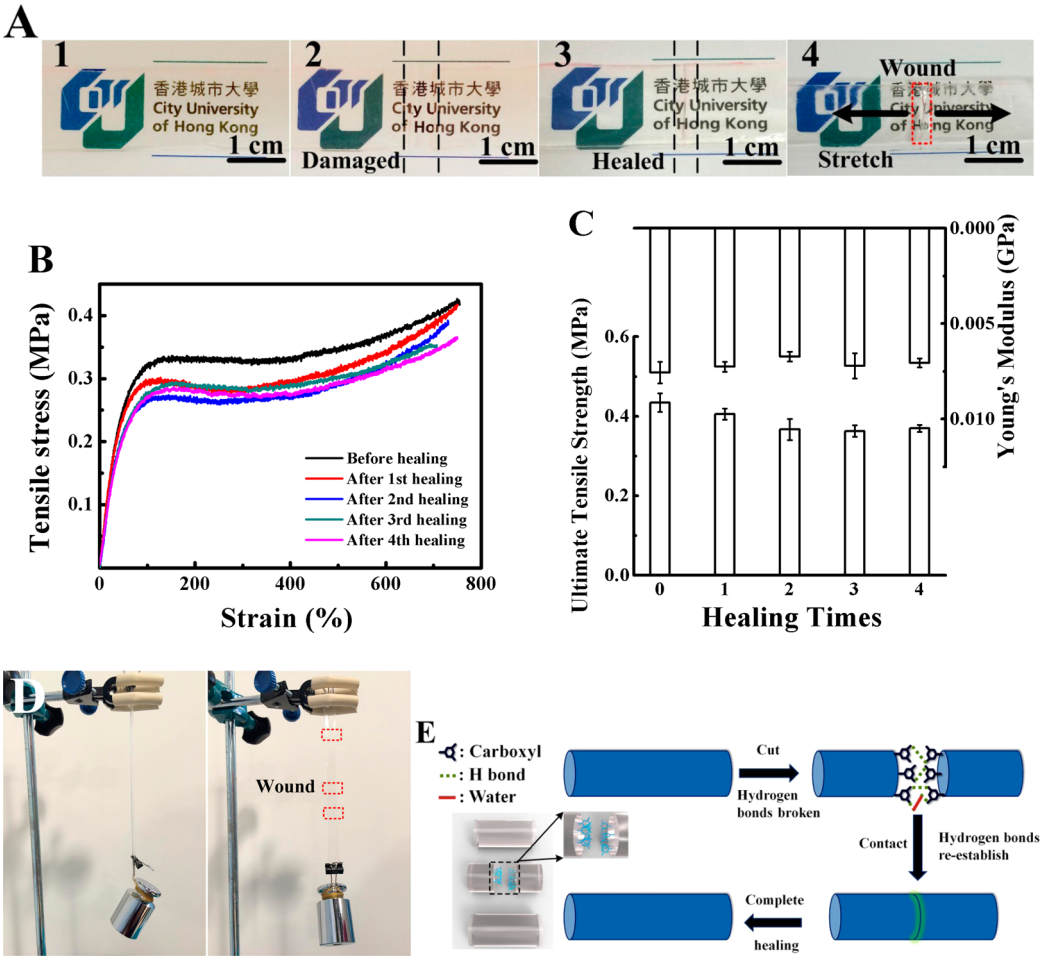

Figure 4. (A) Demonstration of the self-healing process of carboxylated PU: (1) the original PU, (2) after breaking, (3) after self-healing, and (4) stretching after self-healing. The complete self-healing process of a PU film is demonstrated in Supporting Video 2. (B) Tensile measurements of the pure PU after different breaking/healing cycles. (C) Tensile strengths and Young's moduli of the pure PU after different breaking/healing cycles. Mechanical property data of the self-healing PU are averages of three measurements. (D) Demonstration of the self-healing PU (1.07 mm thick and 14.07 mm wide) to completely support a *ca.* 500 g mass, which equates to 0.34 MPa of stress: before healing (left) and after the third breaking/healing cycle (right). Red rectangles indicate the wound/healing positions. (E) Schematic diagram of the self-healing mechanism; inset is a model of the PU rod sample.

surface of the yarn is clean and smooth. After several MW-H treatments, a layer of Fe_3O_4 particles is successfully grown on most of the surface of the yarn. These numerous magnetic particles make the surface rough, which stays the same after the annealing treatment (Figure 3C,D). From the aforementioned photograph (Figure 2C), the appearance of the yarns is not different between the annealed and electrodeposition treatments. However, at the microlevel, their morphologies are totally different. Once PPy is electrodeposited on

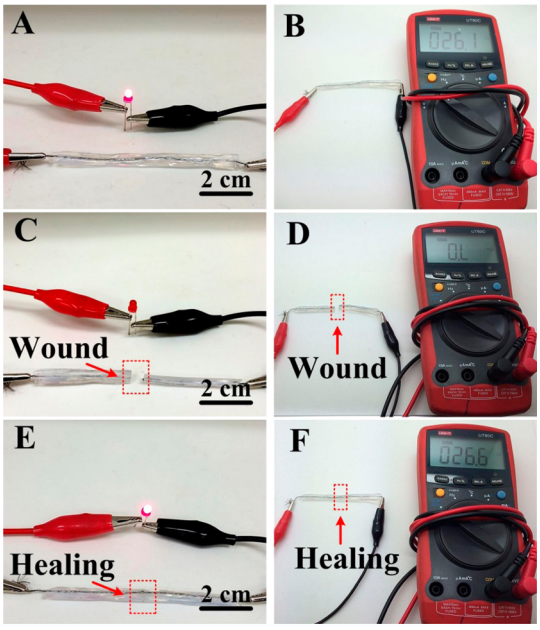

Figure 5. Self-healing electrical conductivity of the as-prepared magnetic electrode wrapped by the self-healing substrate. (A, C, E) Photographs of a self-healing shell wrapped electrode within a circuit with an LED bulb before breaking, after breaking, and after healing. The voltage is set as 3.0 V. (B, D, F) Electrical resistance of a self-healing shell wrapped electrode before breaking, after breaking, and after healing. The unit of the resistance displayed on the multimeter is Ω.

the yarn, the Fe_3O_4 particles are all wrapped tightly by this conducting polymer, leading to a smoother surface, as demonstrated in the high-resolution image (Figure 3E). It is worth noting that PPy acts as not only the active material but also a protecting shell to prevent the important magnetic Fe_3O_4 layer from falling off during practical applications.

Self-Healing PU. Carboxylated PU, composed of a chain of organic units joined by a urethane link (see the chemical structure in Figure S1 of the Supporting Information), served as the outmost self-healing shell in our unique device, which is responsible for the mechanical self-healing. A refined PU belt (fabricated by the drop-casting method) is applied to demonstrate its superior self-healing property, as shown in Figure 4A. First, the PU is bisected using scissors; the fresh wounds of the two pieces are neat, dry, and nonstick, indicating that the self-healing process should not be a simple self-adhering process. Then the cut ends are rejoined under a gentle pressure within tens of seconds and allowed to stand for around 5 min at room temperature. After the wounds are successfully healed, only a linear scar is left on the surface and amazingly the healed PU belt could be stretched hard without breaking. The complete self-healing process of a PU film is demonstrated in Supporting Video 2 (the video runs at 8 times the normal speed).

The mechanical properties of the PU before breaking and after self-healing are systematically investigated, as shown in Figure 4C. From similar variations of the stress−stain curves, it is obvious that the mechanical properties are restored after multiple breaking/self-healing cycles. The tensile strength is well maintained at approximately 84% after the fourth healing, and the Young's modulus is maintained at 86%. Such superior self-healing properties can meet the tough mechanical requirements under extreme conditions (Figure 4D). This outstanding mechanical self-healing benefits from the assembly of supramolecules, which forms both chains and cross-links *via* countless reversible hydrogen bond acceptors and donors. When breakage occurs in the PU, the strong intermolecular hydrogen bonds are broken at the same time. However, this intermolecular hydrogen bonding at the interface is reversible and could re-establish when the fragments are brought into contact, as shown schematically in Figure 4E.[26,30,33,34] Besides, it is reported that the self-healing process could be assisted underwater by the formation of extra interfacial hydrogen bonds,[30] which is also suitable for our PU. A few drops of water (around 200 μL) improve its self-healing property by increasing the hydrogen bonds in the self-healing region (Figure 4E). According to its amazing self-healing power, PU is used as the outmost layer of our supercapacitor.

Self-Healing Supercapacitor. After the electrodeposited magnetic yarn is wrapped with the solid electrolyte and the PU self-healing shell, the self-healing capacity in regard to the electrical conductivity as one as-prepared electrode is investigated. Figure 5A,C,E demonstrates an effective application of the self-healing electrode as a conducting wire in a tandem circuit, which is monitored by a common commercial light-emitting diode (LED). The LED bulb successfully lights up at a voltage of 3.0 V. After breaking of the self-healing electrode, the lighted LED bulb extinguishes immediately. Then, the two halves of the bisected electrode are brought into contact by a gentle pressure, and the LED bulb lights up again with a similar brightness after self-healing of the electrode. The resistance of the electrode is also traced by a multimeter, as shown in Figure 5B,D,F. Apparently, the resistance slightly increases to 26.6 Ω, almost the same value as the one before self-healing (26.1 Ω). Such outstanding healable electrical conductivity should be resultant from both the PU shell and the magnetic layer. Like the aforementioned advantages, the PU guarantees self-healing of the wounds, while the magnetic layer ensures the reconnection of the broken electrode. This synergistic effect is the key design of our self-healable yarn-based supercapacitor.

In order to further prove the synergistic effect of magnetic electrodes and the self-healing shell, the electrochemical performance of a magnetic-assisted self-healable supercapacitor based on our design is

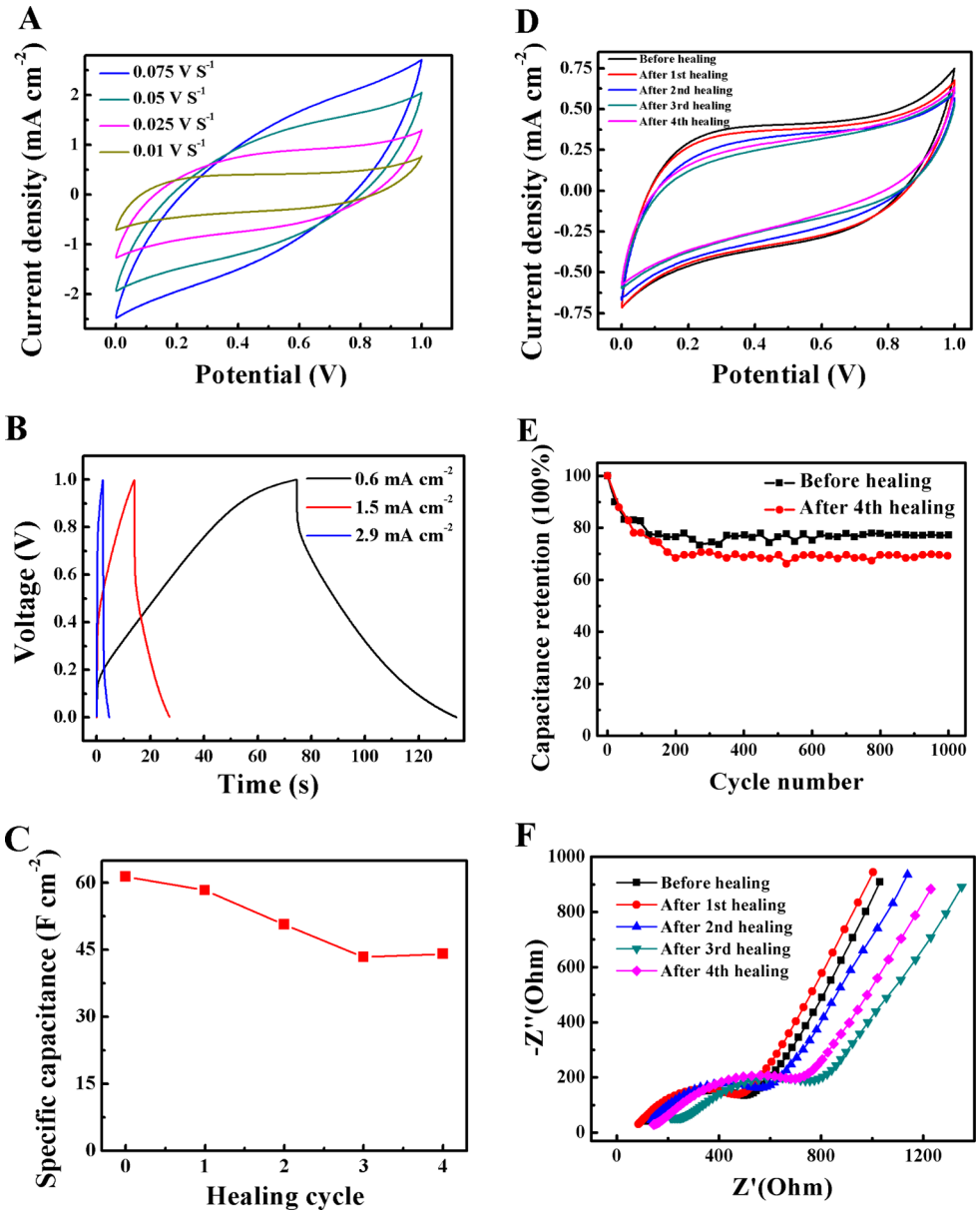

Figure 6. Electrochemical measurements for the as-prepared capacitor. (A) CVs obtained at various scan rates. (B) Galvonostatic charge–discharge measurements of the self-healing supercapacitor at different current densities. (C) Specific capacitance of the original device and after healing for different cycles. (D) CVs after healing for different cycles. (E) Capacitance retention of the device before breaking and after the fourth healing for 1000 cycles under a current density of 4.4 mA cm^{-2}. (F) Nyquist plots of the original device and after self-healing for different cycles.

systematically investigated. A series of rate-dependent cyclic voltammetry (CV) curves of the device in the voltage window from 0 to 1.0 V are shown in Figure 6A. The CV curves are not highly symmetric, owing to the combined effects of the used materials and the special yarn structure. The nonrectangular curves of iron oxides[13,35] and rectangular curves of PPy[14] make the overall CV curves close to rectangular. In addition, the one-dimentional yarn structure composed of multiple tiny fibers has a long length and a small cross section area. Thus, the resistance is higher than that of two- and three-dimentional structures. The capacitance of the yarn electrode is further evaluated by galvanostatic charge/discharge tests at different current densities between 0 and 1 V. The deviation of charge–discharge curves from the linear voltage–time relation for pure double-layer supercapacitors reveals pseudocapacitive behavior resulting from surface-confined Faradaic reaction of the electrodes.[36,37] The specific capacitance of the self-healing device estimated from the CV curve is 61.4 mF cm^{-2} at a scan rate of 10 mV s^{-1},[38,39] which is comparable with other yarn- or fiber-based supercapacitors reported before.[40,41] It is worth noting that after several cycles of cutting/healing the capacitance is still maintained at an amazingly high level. As shown in Figure 6C and Table 1, the specific capacitances

TABLE 1. Electrical Performance of the Self-Healing Supercapacitor before Breaking and after Self-Healing

healing times	specific capacitance [F cm^{-2}][a]	charge-transfer resistance R_{ct} [Ω]	system resistance R_s [Ω]
0	61.4	450.75	35.95
1st	58.3	450.95	37.55
2nd	50.7	508.05	48.85
3rd	43.4	639	80.17
4th	44.1	605.69	75.71

[a] The specific capacitance of the self-healing device is calculated at 10 mV s^{-1}.

calculated from the CV curves of the second and fourth healings are 50.7 and 44.1 mF cm^{-2}, respectively, and the capacitance retention ratio is 71.8% after the fourth healing. Interestingly, the electrical performance of the fourth healing cycle is slightly better than the third cycle. This could be attributed to the adjustment between the broken electrodes, because during the breaking/healing cycles the device unavoidably experienced vigorous manipulation. Because the broken electrodes were reconnected by the self-healing PU and magnetic force, the macroscopical operation would cause the microcosmic adjustment of the reconnected electrodes, resulting in a little fluctuation of the electrical performance during the breaking/healing cycles. Even though the capacitances decrease to some degree after several cycles of cutting and healing, the CV curves remain largely rectangular even after the fourth healing (Figure 6D). This is consistent with the charge/discharge test results as shown in Figure S2, suggesting the redox reactions are not affected after self-healing. To further characterize the cyclability and performance durability of the device before breaking and after healing, galvanostatic charge/discharge tests are carried out up to 1000 cycles at a current density of 4.4 mA cm^{-2}, as shown in Figure 6E. A 23% decay in specific capacitance is observed prior to cutting and a 30% decay after the fourth healing, indicating the good healing performance. Apparently, most of the degradation occurs in the first 200 cycles for both the original and complete healing device, while nearly no degradation is observed in the rest of the cycles. This suggests a fast volumetric change during repeated redox cycles.[42] The cycling stability reported here is better than other PPy-coated fabrics, for example, PPy-coated nylon Lycra fabric (42% decay in the first 200 cycles).[37,43]

Electrochemical impedance spectroscopy (EIS) analysis has been recognized as one of the principle methods to examine the fundamental behaviors of supercapacitors.[43] For a further understanding, the impedance of the self-healing supercapacitor before breaking and after multiple cycles of self-healing is measured in the frequency range of 10^{-1} to 10^5 Hz with a 5 mV amplitude (Figure 6F). The impedance

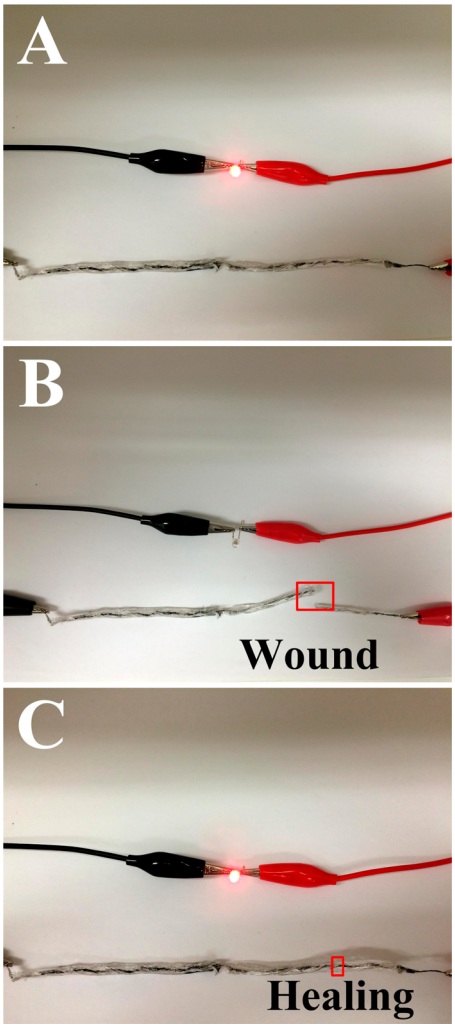

Figure 7. Photographs of two supercapacitors connected in series to power an LED bulb. Each one is coated with a 1 mm thick self-healable PU shell: (A) before breaking, (B) after breaking, and (C) after healing.

spectra are mixed together before and after the healing cycles, which could be attributed to the fine adjustment of the broken electrodes during the manipulation. They are also similar in form, with an arc at a higher frequency region and a spike at lower frequency, demonstrating the electrical stability after multiple cycles of self-healing. The charge-transfer resistances (R_{ct}) of the capacitors before breaking and after the second and fourth healing are 450.75, 508.05, and 605.69 Ω, respectively, consistent with the increase of system resistance (R_s) from 35.95 Ω to 48.85 and 75.71 Ω (Table 1). These results indicate that the resistances increase after healing, owing to the not fully reconnected tiny fibers in the yarn electrodes.

Figure 7 shows the self-healing supercapacitors connected in series to power an LED bulb. Before breaking, the supercapacitors light up the LED successfully, and without doubt the LED extinguishes immediately after breaking. As expected, the LED is lit up

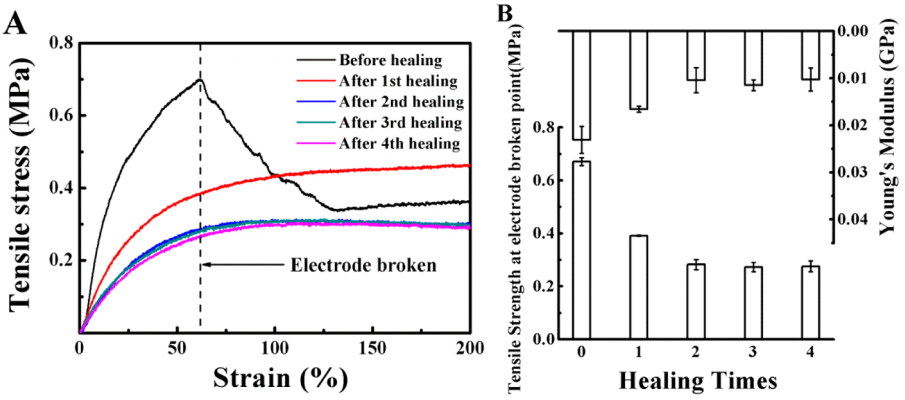

Figure 8. (A) Tensile measurements of the self-healing supercapacitor after different self-healing cyles. (B) Tensile strengths and Young's moduli of the original device and after self-healing for different cycles. Tensile strength is calculated based on the electrode breaking point. It should be noted that before the first breaking, the values of tensile strength and Young's modulus are dominated by the yarn, and after self-healing, these values are dominated by PU. This results in the sudden drops of the values after the first self-healing.

again with almost the same brightness after the broken supercapacitor is reconnected and self-healed. The current passing through the LED bulb at each step is shown in Figure S3. For both the single electrode and the device, the current after reconnection is a bit lower than that before reconnection due to the resistance increase. As mentioned above, the remarkable performance after self-healing is based on the synergistic effect of the PU shell and magnetic electrodes, as illustrated in Figure 1B. Figure 8 shows the mechanical properties of the whole device before and after healing. The sudden drop of the mechanical properties after the first healing process is due to the strength difference between the yarn and PU. That is, before the cutting−healing cycles, the high Young's modulus and strength are attributed to the great mechanical performances of the yarn, while after the first cutting, the mechanical properties are dominated by those of the PU. It is reasonable that the magnetic force is helpful for reconnection of the electrodes, but its contribution to mechanical strength is very limited. After the first breaking of the electrodes, the mechanical properties with different breaking/healing cycles are maintained very well and close to those of the pristine PU, showing that the self-healing PU shell is effective. This guarantees enough mechanical strength after self-healing, which is favorable for practical applications.

CONCLUSIONS

In conclusion, an electrically and mechanically self-healable yarn-based supercapacitor is designed and fabricated by wrapping magnetic electrodes with a self-healing carboxylated PU shell. The magnetic force assists the broken electrode's reconnection through magnetic alignment, which benefits the recovery of electrochemical performance after self-healing. Meanwhile, the carboxylated PU shell is responsible for the outstanding mechanically self-healing performance, which is crucial for practical applications. Due to the synergistic effect of the magnetic electrodes and the self-healing shell, the yarn-based supercapacitor exhibits an excellent self-healing performance: the specific capacitance is restored to 71.8% after the fourth healing. In addition, the mechanical properties of the whole device can be well maintained after multiple cutting−healing cycles. The self-healable yarn supercapacitor as fabricated provides a solution to extend the lifespan of wearable electronics, meeting the requirement of sustainability. This work may enlighten the design and fabrication of various self-healable and wearable electronics in the near future.

EXPERIMENTAL SECTION

Reagents and Materials. Iron (II) chloride ($FeCl_2$), urea, poly(vinyl alcohol) (PVA), pyrrole, polyurethane, *p*-toluenesulfonic acid, sodium dodecylbenzenesulfonate, phosphoric acid (H_3PO_4), acetone, methanol, and ethanol are analytical grade. Pyrrole was freshly distilled before use, and polyurethane was modified by carboxyl groups. Multiple stainless steel fibers were twist-drawn to form yarns through a collaboration with Kezhengyuan Yarn Company. PU is modified as carboxylated PU, which is soluble in water.

Preparation of Magnetic Yarn Electrode. The stainless steel yarn with appropriate length (10−15 cm) was sonicated in acetone and methanol for 30 min and then washed with deionized water (DW) and dried prior to use. Then 500 mg of $FeCl_2$ and 2.8 g of urea were dissolved in 30 mL of DW to form a pale yellow solution. The cleaned and dried yarn was bathed in this solution and sonicated for 30 min. Then both the solution and the yarn were transferred into a 100 mL Teflon-lined double-walled digestion vessel and heated at 160 °C for 30 min in a microwave digestion system (MDS-6G, Shanghai Sineo Microwave Chemistry Technology Co., Ltd.). After the vessel was taken out and cooled to room temperature, the black yarn was taken out and washed with DW gently and dried prior to use; the black residual powder was collected by centrifugation, rinsed with DW and

absolute ethanol several times, and dried at 80 °C overnight. The dried black yarn was annealed at 250 °C under air flow for 1 h with a ramp rate of 5 °C/min. As a result, the black magnetic yarn was successfully prepared. PPy was electrodeposited on the surface of the black magnetic yarn. Briefly, the electrodeposition solution contained 300 μL of distilled pyrrole monomer, 0.1 M *p*-toluenesulfonic acid, 0.3 M sodium dodecylbenzenesulfonate, and 60 mL of DW. A three-electrode configuration was used in the deposition process with the annealed magnetic yarn as working electrode, platinum wire as counter electrode, and Ag/AgCl as reference electrode. A constant voltage of 0.8 V was used during the deposition process, and the temperature was kept at 0 °C. Then the as-prepared PPy-wrapped magnetic electrode was washed in DW and dried prior to use.

Fabrication of Magnetic-Assisted, Self-Healing, Yarn-Based Supercapacitor. The PVA-H_3PO_4 gel electrolyte was first prepared by dissolving PVA powder (6 g) in DW (60 mL) and H_3PO_4 (3.54 mL). The mixture was heated to 90 °C with continuous stirring until a transparent solution formed. Two PPy-wrapped magnetic electrodes were coated with the PVA-H_3PO_4 gel electrolyte and dried under vacuum at room temperature. The resultant two solid-electrolyte-wrapped electrodes were twisted together, followed by coating another layer of electrolyte, and dried under vacuum. Finally, the PU was coated on the supercapacitor and dried in air. For the characterization of self-healing properties, the pure PU belt and the supercapacitor were cut, followed by contacting the broken sections together.

Characterization. Structural and phase characterizations of the residual powder were done by XRD using a Bruker D2 Phaser diffractometer with Cu Kα irradiation (λ = 1.54 Å). The surface morphology of the yarns after different treatments was characterized by an environmental scanning electron microscope (ESEM, FEI/Philips XL30). Electrochemical measurements including cyclic voltammetry curves, galvanostatic charge/discharge curves, and electrochemical impedance spectroscopy (100 kHz to 0.1 Hz) were conducted by an electrochemical workstation (CHI 760D). The stress–strain curves were conducted on a Zwick Z030 tester (tensile rate = 50 mm min^{-1}). During the mechanical strength tests, the pure PU samples had the same size and shape as the self-healing supercapactior. Sample widths were measured by vernier calipers, and the thickness was measured in micrometers. The sample size was measured at least three times at different positions to take the average.

Calculations of Specific Capacitance. The areal specific capacitance (C) in two-electrode configuration was calculated from the corresponding CV curves at different scan rates according to the equation[38,39]

$$C = \frac{1}{s\nu\Delta V}\int_{V_0}^{V_0+\Delta V} I dV \qquad (1)$$

where I (A) is the response current, ν is the scan rate (V s^{-1}), s is the surface area of the electrode (cm^2), V_0 is the lower potiential limit, and ΔV is the potential window (V). The surface area of the electrode s is calculated based on the following equation: $s = \pi dL$, where d is the diameter of the electrode (cm) and L is the length of the electrode wrapped with the solid electrolyte (cm).

Conflict of Interest: The authors declare no competing financial interest.

Acknowledgment. This research was partially supported by the Early Career Scheme of the Research Grants Council of Hong Kong SAR, China, under Project No. 109213, and the Science Technology and Innovation Committee of Shenzhen Municipality (Grant No. JCYJ20130401145617276). The authors would like to thank Mr. T. F. Hung and Mr. T. W. Chan in the Department of Physics and Materials Science of the City University of Hong Kong for several measurements.

Supporting Information Available: The Supporting Information is available free of charge on the ACS Publications website at DOI: 10.1021/acsnano.5b01602.

REFERENCES AND NOTES

1. Xu, Y.; Lin, Z.; Huang, X.; Liu, Y.; Huang, Y.; Duan, X. Flexible Solid-State Supercapacitors Based on Three-Dimensional Graphene Hydrogel Films. *ACS Nano* **2013**, *7*, 4042–4049.
2. Xie, K.; Wei, B. Materials and Structures for Stretchable Energy Storage and Conversion Devices. *Adv. Mater.* **2014**, *26*, 3592–3617.
3. Zhong, J.; Zhang, Y.; Zhong, Q.; Hu, Q.; Hu, B.; Wang, Z. L.; Zhou, J. Fiber-Based Generator for Wearable Electronics and Mobile Medication. *ACS Nano* **2014**, *8*, 6273–6280.
4. Shim, B. S.; Chen, W.; Doty, C.; Xu, C.; Kotov, N. A. Smart Electronic Yarns and Wearable Fabrics for Human Biomonitoring Made by Carbon Nanotube Coating with Polyelectrolytes. *Nano Lett.* **2008**, *8*, 4151–4157.
5. Liu, N.; Ma, W.; Tao, J.; Zhang, X.; Su, J.; Li, L.; Yang, C.; Gao, Y.; Golberg, D.; Bando, Y. Cable-Type Supercapacitors of Three-Dimensional Cotton Thread Based Multi-Grade Nanostructures for Wearable Energy Storage. *Adv. Mater.* **2013**, *25*, 4925–4931.
6. Liu, D.; Wang, X.; Wang, X.; Tian, W.; Liu, J.; Zhi, C.; He, D.; Bando, Y.; Golberg, D. Ultrathin Nanoporous Fe_3O_4-Carbon Nanosheets with Enhanced Supercapacitor Performance. *J. Mater. Chem. A* **2013**, *1*, 1952–1955.
7. Tao, J.; Liu, N.; Ma, W.; Ding, L.; Li, L.; Su, J.; Gao, Y. Solid-State High Performance Flexible Supercapacitors Based on Polypyrrole-MnO_2-Carbon Fiber Hybrid Structure. *Sci. Rep.* **2013**, *3*, 2286.
8. Zhang, D.; Miao, M.; Niu, H.; Wei, Z. Core-Spun Carbon Nanotube Yarn Supercapacitors for Wearable Electronic Textiles. *ACS Nano* **2014**, *8*, 4571–4579.
9. Kou, L.; Huang, T.; Zheng, B.; Han, Y.; Zhao, X.; Gopalsamy, K.; Sun, H.; Gao, C. Coaxial Wet-Spun Yarn Supercapacitors for High-Energy Density and Safe Wearable Electronics. *Nat. Commun.* **2014**, *5*, 3754.
10. Choi, C.; Lee, J. A.; Choi, A. Y.; Kim, Y. T.; Lepró, X.; Lima, M. D.; Baughman, R. H.; Kim, S. J. Flexible Supercapacitor Made of Carbon Nanotube Yarn with Internal Pores. *Adv. Mater.* **2014**, *26*, 2059–2065.
11. Tian, W.; Wang, X.; Zhi, C.; Zhai, T.; Liu, D.; Zhang, C.; Golberg, D.; Bando, Y. $Ni(OH)_2$ Nanosheet @ Fe_2O_3 Nanowire Hybrid Composite Arrays for High-Performance Supercapacitor Electrodes. *Nano Energy* **2013**, *2*, 754–763.
12. Zhu, J.; Cao, L.; Wu, Y.; Gong, Y.; Liu, Z.; Hoster, H. E.; Zhang, Y.; Zhang, S.; Yang, S.; Yan, Q.; Ajayan, P. M.; Vajtai, R. Building 3D Structures of Vanadium Pentoxide Nanosheets and Application as Electrodes in Supercapacitors. *Nano Lett.* **2013**, *13*, 5408–5413.
13. Meng, W.; Chen, W.; Zhao, L.; Huang, Y.; Zhu, M.; Huang, Y.; Fu, Y.; Geng, F.; Yu, J.; Chen, X.; Zhi, C. Porous Fe_3O_4/Carbon Composite Electrode Material Prepared from Metal-Organic Framework Template and Effect of Temperature on its Capacitance. *Nano Energy* **2014**, *8*, 133–140.
14. Huang, Y.; Tao, J.; Meng, W.; Zhu, M.; Huang, Y.; Fu, Y.; Gao, Y.; Zhi, C. Super-High Rate Stretchable Polypyrrole-Based Supercapacitors with Excellent Cycling Stability. *Nano Energy* **2015**, *11*, 518–525.
15. He, Y.; Chen, W.; Li, X.; Zhang, Z.; Fu, J.; Zhao, C.; Xie, E. Freestanding Three-Dimensional Graphene/MnO_2 Composite Networks as Ultralight and Flexible Supercapacitor Electrodes. *ACS Nano* **2012**, *7*, 174–182.
16. Hu, L.; Chen, W.; Xie, X.; Liu, N.; Yang, Y.; Wu, H.; Yao, Y.; Pasta, M.; Alshareef, H. N.; Cui, Y. Symmetrical MnO_2–Carbon Nanotube–Textile Nanostructures for Wearable Pseudocapacitors with High Mass Loading. *ACS Nano* **2011**, *5*, 8904–8913.
17. Wang, Q.; Wang, X.; Xu, J.; Ouyang, X.; Hou, X.; Chen, D.; Wang, R.; Shen, G. Flexible Coaxial-Type Fiber Supercapacitor Based on $NiCo_2O_4$ Nanosheets Electrodes. *Nano Energy* **2014**, *8*, 44–51.
18. Liu, N.; Li, J.; Ma, W.; Liu, W.; Shi, Y.; Tao, J.; Zhang, X.; Su, J.; Li, L.; Gao, Y. Ultrathin and Lightweight 3D Free-Standing Ni@NiO Nanowire Membrane Electrode for a Supercapacitor with Excellent Capacitance Retention at High Rates. *ACS Appl. Mater. Interfaces* **2014**, *6*, 13627–13634.

19. Zhang, Q.; Scrafford, K.; Li, M.; Cao, Z.; Xia, Z.; Ajayan, P. M.; Wei, B. Anomalous Capacitive Behaviors of Graphene Oxide Based Solid-State Supercapacitors. *Nano Lett.* **2014**, *14*, 1938–1943.
20. Chan, C. K.; Peng, H.; Liu, G.; McIlwrath, K.; Zhang, X. F.; Huggins, R. A.; Cui, Y. High-Performance Lithium Battery Anodes Using Silicon Nanowires. *Nat. Nanotechnol.* **2008**, *3*, 31–35.
21. Chen, Y.-C.; Hsu, Y.-K.; Lin, Y.-G.; Lin, Y.-K.; Horng, Y.-Y.; Chen, L.-C.; Chen, K.-H. Highly Flexible Supercapacitors with Manganese Oxide Nanosheet/Carbon Cloth Electrode. *Electrochim. Acta* **2011**, *56*, 7124–7130.
22. Huang, L.; Yi, N.; Wu, Y.; Zhang, Y.; Zhang, Q.; Huang, Y.; Ma, Y.; Chen, Y. Multichannel and Repeatable Self-Healing of Mechanical Enhanced Graphene-Thermoplastic Polyurethane Composites. *Adv. Mater.* **2013**, *25*, 2224–2228.
23. Wang, X.; Lu, X.; Liu, B.; Chen, D.; Tong, Y.; Shen, G. Flexible Energy-Storage Devices: Design Consideration and Recent Progress. *Adv. Mater.* **2014**, *26*, 4763–4782.
24. Burattini, S.; Greenland, B. W.; Chappell, D.; Colquhoun, H. M.; Hayes, W. Healable Polymeric Materials: A Tutorial Review. *Chem. Soc. Rev.* **2010**, *39*, 1973–1985.
25. Wietor, J.-L.; Sijbesma, R. P. A Self-Healing Elastomer. *Angew. Chem., Int. Ed.* **2008**, *47*, 8161–8163.
26. Wang, H.; Zhu, B.; Jiang, W.; Yang, Y.; Leow, W. R.; Wang, H.; Chen, X. A Mechanically and Electrically Self-Healing Supercapacitor. *Adv. Mater.* **2014**, *26*, 3638–3643.
27. Sun, H.; You, X.; Jiang, Y.; Guan, G.; Fang, X.; Deng, J.; Chen, P.; Luo, Y.; Peng, H. Self-Healable Electrically Conducting Wires for Wearable Microelectronics. *Angew. Chem., Int. Ed.* **2014**, *126*, 9680–9685.
28. Huang, Y.; Hu, H.; Huang, Y.; Zhu, M.; Meng, W.; Pei, Z., Liu, C. From Industrially Weavable and Knittable Highly Conductive Yarns to Large Wearable Energy Storage Textiles. *ACS Nano* **2015**, *9*, 4766−4775.
29. Armao, J. J.; Maaloum, M.; Ellis, T.; Fuks, G.; Rawiso, M.; Moulin, E.; Giuseppone, N. Healable Supramolecular Polymers as Organic Metals. *J. Am. Chem. Soc.* **2014**, *136*, 11382–11388.
30. Ahn, B. K.; Lee, D. W.; Israelachvili, J. N.; Waite, J. H. Surface-Initiated Self-Healing of Polymers in Aqueous Media. *Nat. Mater.* **2014**, *13*, 867–872.
31. Du, P.; Wu, M.; Liu, X.; Zheng, Z.; Wang, X.; Joncheray, T.; Zhang, Y. Diels−Alder-Based Crosslinked Self-Healing Polyurethane/Urea from Polymeric Methylene Diphenyl Diisocyanate. *J. Appl. Polym. Sci.* **2014**, *131*, 40234–40240.
32. Babanejad, N.; Nikjeh, M. M. A.; Amini, M.; Dorkoosh, F. A. A Nanoparticulate Raloxifene Delivery System Based on Biodegradable Carboxylated Polyurethane: Design, Optimization, Characterization, and *in Vitro* Evaluation. *J. Appl. Polym. Sci.* **2014**, *131*, 393668–39677.
33. Tee, B. C. K.; Wang, C.; Allen, R.; Bao, Z. An Electrically and Mechanically Self-Healing Composite with Pressure- and Flexion-Sensitive Properties for Electronic Skin Applications. *Nat. Nanotechnol.* **2012**, *7*, 825–832.
34. Zhang, H.; Xia, H.; Zhao, Y. Poly(vinyl alcohol) Hydrogel Can Autonomously Self-Heal. *ACS Macro Lett.* **2012**, *1*, 1233–1236.
35. Yang, P.; Ding, Y.; Lin, Z.; Chen, Z.; Li, Y.; Qiang, P.; Ebrahimi, M.; Mai, W.; Wong, C. P.; Wang, Z. L. Low-Cost High-Performance Solid-State Asymmetric Supercapacitors Based on MnO_2 Nanowires and Fe_2O_3 Nanotubes. *Nano Lett.* **2014**, *14*, 731–736.
36. Kong, L.-B.; Liu, M.; Lang, J.-W.; Luo, Y.-C.; Kang, L. Asymmetric Supercapacitor Based on Loose-Packed Cobalt Hydroxide Nanoflake Materials and Activated Carbon. *J. Electrochem. Soc.* **2009**, *156*, A1000–A1004.
37. Yue, B.; Wang, C.; Ding, X.; Wallace, G. G. Polypyrrole Coated Nylon Lycra Fabric as Stretchable Electrode for Supercapacitor Applications. *Electrochim. Acta* **2012**, *68*, 18–24.
38. Liu, J.; Zhang, L.; Wu, H. B.; Lin, J.; Shen, Z.; Lou, X. W. High-Performance Flexible Asymmetric Supercapacitors Based on A New Graphene Foam/Carbon Nanotube Hybrid Film. *Energy Environ. Sci.* **2014**, *7*, 3709–3719.
39. Yu, D.; Goh, K.; Wang, H.; Wei, L.; Jiang, W.; Zhang, Q.; Dai, L.; Chen, Y. Scalable Synthesis of Hierarchically Structured Carbon Nanotube-Graphene Fibres for Capacitive Energy Storage. *Nat. Nanotechnol.* **2014**, *9*, 555–562.
40. Lee, J. A.; Shin, M. K.; Kim, S. H.; Cho, H. U.; Spinks, G. M.; Wallace, G. G.; Lima, M. D.; Lepró, X.; Kozlov, M. E.; Baughman, R. H.; Kim, S. J. Ultrafast Charge and Discharge Biscrolled Yarn Supercapacitors for Textiles and Microdevices. *Nat. Commun.* **2013**, *4*, 1970.
41. Le, V. T.; Kim, H.; Ghosh, A.; Kim, J.; Chang, J.; Vu, Q. A.; Pham, D. T.; Lee, J.-H.; Kim, S.-W.; Lee, Y. H. Coaxial Fiber Supercapacitor Using All-Carbon Material Electrodes. *ACS Nano* **2013**, *7*, 5940–5947.
42. Liu, T.; Finn, L.; Yu, M.; Wang, H.; Zhai, T.; Lu, X.; Tong, Y.; Li, Y. Polyaniline and Polypyrrole Pseudocapacitor Electrodes with Excellent Cycling Stability. *Nano Lett.* **2014**, *14*, 2522–2527.
43. Lee, H.; Kim, H.; Cho, M. S.; Choi, J.; Lee, Y. Fabrication of Polypyrrole (PPy)/Carbon Nanotube (CNT) Composite Electrode on Ceramic Fabric for Supercapacitor Applications. *Electrochim. Acta* **2011**, *56*, 7460–7466.